Electronic Supplementary Material (ESI) for Nanoscale Horizons.

Supporting Information

Size dependent surface reconstruction in detonation nanodiamond

Shery L.Y. Chang

Leroy Eyring Center for Solid State Science,

Arizona State University, Tempe, USA

Christian Dwyer

Department of Physics, Arizona State University, Tempe, USA

Eiji Ōsawa

NanoCarbon Research Institute, Ueda, Japan

Amanda S. Barnard

Data61, CSIRO, Docklands, Australia.

A. Synthesis of dispersed elementary particles of detonation nanodiamond and surface chemistry characterisations

Commercial crude products of detonation nanodiamond were purchased from Comstar Technology Limited, Hong Kong. This material is composed of large and extremely tight agglutinates of the elementary particles of DND, and disintegrated by means of attrition milling. The milling and work-up consist of suspending the as-received agglutinates in water by high-speed agitation, circulating the suspension through a vertical attrition mill equipped with centrifugal separator and connected in series with a 450W vertically vibrating sonication rod to give a black aqueous solution of crude elementary particle of DND. The solution is subjected to refrigerating to separate uncrushed solid contaminants, final centrifugal separation to remove metal oxides and other heavy impurities as precipitates. Supernatant clear but intensely black and slightly viscous aqueous solution is collected by decantation to give monodisperse colloidal elementary particles of DND in water. TEM works reported herein are carried out by transferring droplets from this solution directly to the grid sample holder.

Surface chemistry was measured using FTIR in a transmission mode. The signals contains C-H groups (2800-3000 cm^{-1}), carbonyl groups (about 1730-1750 cm^{-1}), and hydroxyl groups and absorbed water.

B. HRTEM imaging and electron energy loss spectroscopy using monochromated, spherical- (C_s) and chromatic- (C_c) aberration corrected TEM

High-resolution imaging was performed using a spherical- (C_s) and chromatic- (C_c) aberration-corrected TEM (FEI Company) operated at 80 kV. Spherical aberration (C_s) was corrected to -3 μm and (C_c) corrected to 2 μm. This combination gives a spatial resolution of better than 1 Å(theoretical resolution of 0.8 Å). The spatial resolution without C_c correction is about 1.9 Å for 80 kV. It is worth emphasizing here that while there are a handful of publications that show the aberration-corrected HRTEM images of nanodiamond, those were taken without chromatic correction, and therefore the images are at lower resolution (2Å) which could not provide images of well-separated atomic columns of diamond (at least 1Å resolution is needed). In this case, more than 200 HRTEM images were taken

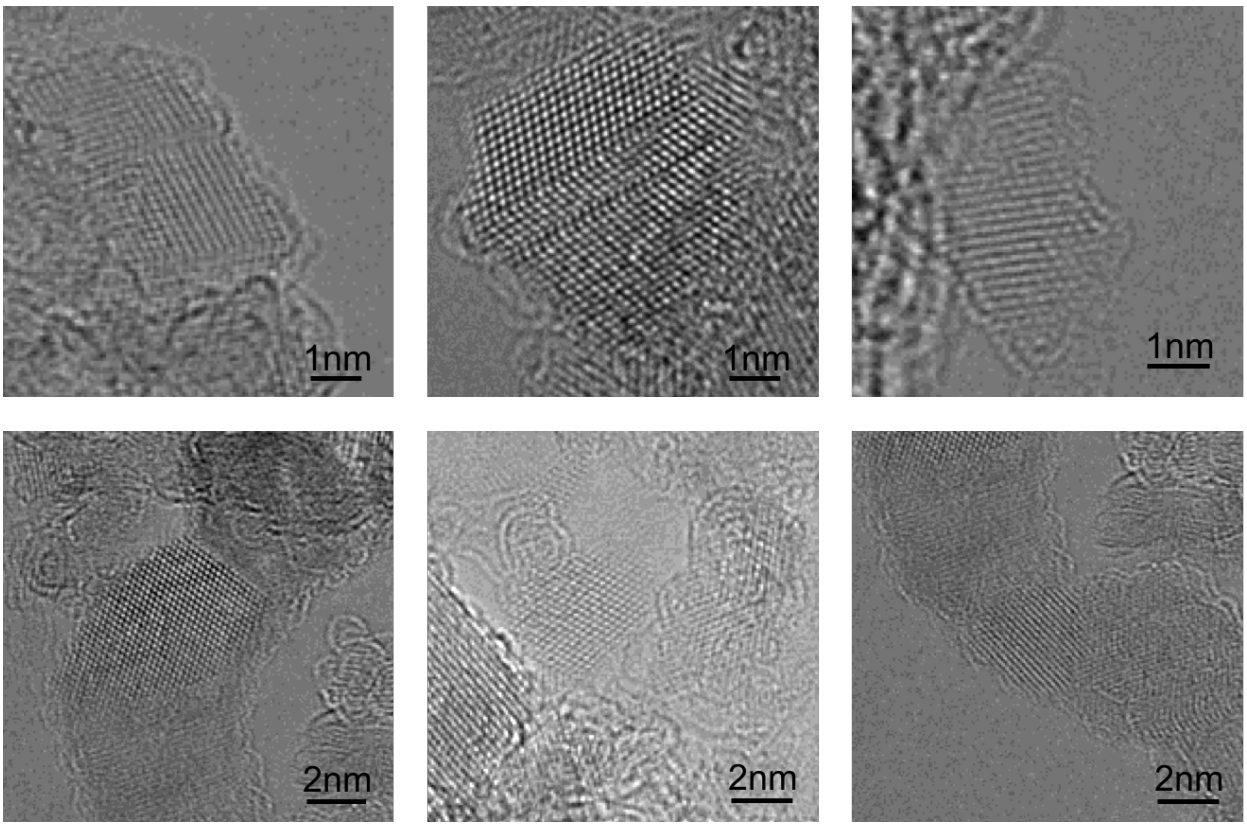

FIG. S1. Selections of high-resolution TEM images of detonation nanodiamond showing their core and surfaces of various sizes, shape and particle orientations.

at negative C_s imaging condition to maximize the contrast of the surface structure, which is only few carbon atoms.. Only nanodiamond particles that are oriented along the zone axis, no (or very little) overlapping with neighbouring particles, and attached over the edge of the supporting holey carbon film of the TEM grid (so that the nanodiamond background contrast is over the vacuum) are selected. This stringent selection is required so that the surface structure as well as the facet size of the particles can be analyzed. Fig. S1 shows a selection of HRTEM images of nanodiamond particles of various sizes, shapes and particle orientations. Common to all particles is that there are diamond cores and the surface structure varies depending on their sizes and shapes. Only the particles that are on zone axis, and the surface atomic structure is fully resolved are selected for showing in the main text and were used for quantitative curvature analysis.

Electron energy loss spectroscopy (EELS) is performed at 80 kV with monochromator excited to give 0.2 eV energy resolution. Dispersion of 50 meV per channel was used to give

optimum signal and spectral features. EELS for DND as well as the reference bulk diamond powder and fullerene were are taken at the same condition. Absolute energy loss and energy dispersion were calibrated quantitatively.

C. HRTEM image simulations

HRTEM image simulations were performed using author-written codes which account for dynamical scattering via multislice theory. Image simulation parameters were chosen according to the experimental conditions, which are the negative C_s imaging condition: accelerating voltage of 80 kV, $C_1 = 5 \pm 2$ nm, $C_s = -3 \pm 1.5$ μm, beam divergence of 0.1 mrad and focal spread of 3 nm.

D. DFTB calculations of nanodiamond particles

The density functional tight-binding method with self-consistent charges (SCC-DFTB), which was implemented in the DFTB+ code [1], was used to perform the calculations [2, 3]. The SCC-DFTB is an approximate quantum chemical approach where the Kohn–Sham density functional is expanded to second order around a reference electron density. The reference density is obtained from self-consistent density functional calculations of weakly confined neutral atoms within the generalized gradient approximation (GGA). The confinement potential is optimized to anticipate the charge density and effective potential in molecules and solids. A minimal valence basis set is used to account explicitly for the two-center tight-binding matrix elements within the DFT level. The double counting terms in the Coulomb and exchange–correlation potential, as well as the intra-nuclear repulsion are replaced by a universal short-range repulsive potential. All structures have been fully relaxed with a conjugate gradient methodology until forces on each atom was minimized to be less than 10^{-4} a.u. (i.e. $\approx$5 meV/Å). In all the calculations, the "PBC" set of parameters is used to describe the contributions from diatomic interactions of carbon.

E. Electronic structure calculations of shape- and size-dependent nanodiamond particles

Using the calculation method described in the previous section, 12 different shapes of nanodiamond particles ranging from 1.7 to 4 nm were calculated. The shapes of the particles contain varying fractions of {111}, {100} and {110} surfaces in accordance with observations in experiments. Fig. S2 shows the shape map of such collections of nanodiamond particles, in which red facets represent {100} surfaces, blue {111} and green {110}. The sp^2, sp^{2+x} and sp^3 fractions for each particle were analyzed. Fig. S3 plotted the sp^2 (grey diamond), sp^{2+x} (blue circle) and sp^3 (red square) fractions for the 12 different shapes up to 4 nm. It can be seen that the sp^{2+x} fraction is strongly dependent on the shapes. For example, octahedron shaped particles (OH) show very little sp^{2+x} fraction changes with varying particle size, whereas cubic particles (HH) show scattered behaviour of sp^{2+x} fraction with no strong correlation with particle size. However particles containing significant fractions of {110} surfaces show more prounced size dependent behaviour, with higher sp^{2+x} fraction with decreasing particle size. Depending on the shape, the sp^{2+x} fraction can vary from 25% to 40$ for particles < 2 nm, and reduces to 13% to 18% when particles increases to 4 nm.

F. Curvature measurements

As the measure of surface curvature we adopt the geometric curvature, which is defined as the normalized tangent vector of the curve. The geometric curvatures of calculated atomic models were measured from the simulated HRTEM images. Curvatures of experimentally observed particles were extracted from the HRTEM images where the atomic columns are resolved (indicated by the red arrows in Fig. 2).

---

[1] B. Aradi, B. Hourahine, and T. Frauenheim, J. Phys. Chem. A **111**, 5678 (2007).

[2] D. Porezag, T. Frauenheim, T. Köhler, G. Seifert, and R. Kaschner, Phys. Rev. B **51**, 12947 (1995).

[3] T. Frauenheim, G. Seifert, M. Elstner, T. Niehaus, C. Köhler, M. Amkreutz, M. Sternberg, Z. Hajnal, A. Di Carlo, and S. Suhai, J. Phys.: Condens. Matter **14**, 3015 (2002).

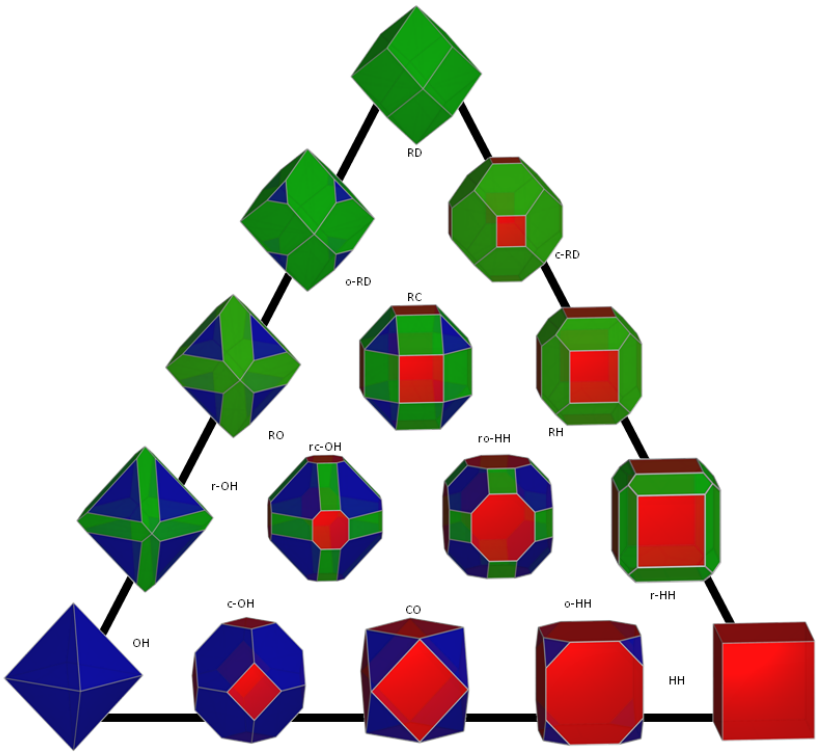

FIG. S2. Shape map of nanodiamond particles consisting of various ratios of {111}, {100} and {110} surfaces.

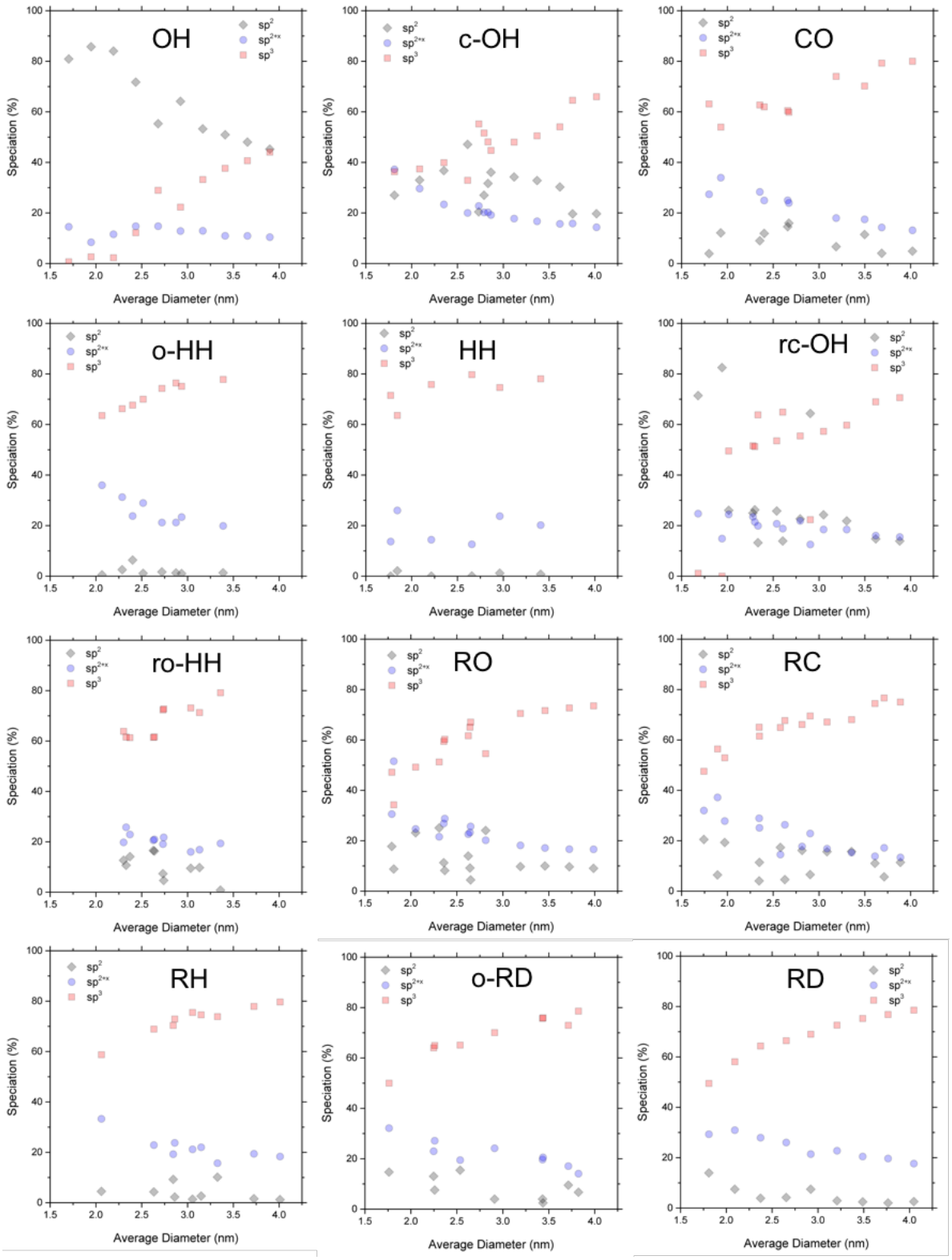

FIG. S3. Fractions of sp^2, sp^{2+x}, and sp^3 plotted for nanodiamond particles of 12 different shapes listed in Fig. S2 with sizes up to 4 nm.